Embedment Length of Steel Coupling Beams—Evaluation and Proposed Revision to the AISC *Seismic Provisions* for Ordinary Composite Coupled Walls

SUSHIL KUNWAR and BAHRAM M. SHAHROOZ

ABSTRACT

One of the composite systems codified in AISC 341 (2022) is composite coupled walls, which are comprised of two or more reinforced concrete structural (shear) walls linked by steel or composite coupling beams embedded in the wall piers. The embedment length is a critical factor that affects the stiffness and strength of the coupling beams—two factors that affect the overall performance of coupled walls. Past studies have examined the performance of special coupled walls in which the wall piers are heavily reinforced and typically have boundary elements. A recent series of tests focused on ordinary composite coupled walls demonstrated that the embedment length determined according to the 2022 edition of AISC 341 was insufficient to develop the target member strength. The results prompted a need to reevaluate the equation by which the embedment length is determined. Using basic principles supported by experimental data, a revised equation was developed and evaluated through numerical simulations. The revised equation results in longer embedment lengths by as much as nearly 40% for cases that would likely be encountered in practice.

Keywords: composite construction, coupling beam, coupled walls, embedment length, structural wall, shear wall.

INTRODUCTION

Coupled structural (shear) walls (CSW) are a common structural system. This system is comprised of two or more structural walls that are typically linked at each floor by coupling beams. Based on the expected level of inelastic deformations, composite structural (shear) walls can be classified as composite ordinary shear walls (C-OSW) or composite special shear walls (C-SSW). One common composite system involves linking reinforced concrete wall piers by steel (or steel-concrete composite) coupling beams that are embedded in the wall piers.

The required embedment length of the coupling beam, L_e, is calculated using Equation H4-4 from AISC 341 (AISC, 2022), hereafter referred to as AISC 341-22, shown here as Equation 1:

$$V_{n,connection} = 1.54\sqrt{f_c'}\left(\frac{b_w}{b_f}\right)^{0.66}\beta_1 b_f L_e\left(\frac{0.58-0.22\beta_1}{0.88+\frac{g}{2L_e}}\right) \quad (1)$$

where

L_e = embedment length of coupling beam measured from the face of the wall, in.
$V_{n,\,connection}$ = design shear strength, kips
b_f = width of beam flange, in.
b_w = thickness of wall, in.
f_c' = specified compressive strength of concrete, ksi
g = clear span of coupling beam, in.
β_1 = factor relating depth of equivalent rectangular compressive stress block to neutral axis depth, as defined by ACI 318-19 (2019)

This equation was developed by Mattock and Gaffar (1982) based on the data from monotonic testing of steel members (acting as brackets) embedded in precast columns. Prior to this study, Marcakis and Mitchell (1980) investigated the performance of precast concrete connections with embedded steel members subjected to monotonic loading. In addition to W-shapes, the embedded steel members in both studies included solid sections or HSS (filled or unfilled).

Including Mattock's and Marcakis's original tests, a database containing the data and results from 52 tests was

Sushil Kunwar, Research and Development Structural Engineer, Browder + LeGuizamon and Associates, Atlanta, Ga. Email: sushil@blaengineers.com (Former Doctoral Research Assistant, Department of CAECM, University of Cincinnati)

Bahram M. Shahrooz, Professor Emeritus, Department of CAECM, University of Cincinnati, Cincinnati, Ohio. Email: bahram.shahrooz@uc.edu (corresponding)

Paper No. 2024-05R

Table 1. Summary of Key Aspects of Available Research Data						
Source	Number of Specimens	Loading	f'_c (ksi)	$\frac{g}{2d}$	$\frac{L_e}{d}$	Controlling Limit State
Marcakis and Mitchell (1980)*+	18	Monotonic	3.40–5.80	1.8–2.0	1.00-1.50	Connection strength
Mattock and Gaffar (1982)+	5	Monotonic	2.95–4.10	1.0–2.7	1.33-2.25	Connection strength
Shahrooz et al. (1993)*	3	Cyclic	4.82–5.62	2.2–2.3	1.89	Coupling beam M_p
Harries (1995)	4	Cyclic	3.75–6.25	1.3–3.5	1.43-1.73	Coupling beam M_p or V_p
Fortney (2005)*	3	Cyclic	5.13–5.30	2.6	2.18	Coupling beam V_p
Park et al. (2005) and Park and Yun (2006)*	9	Cyclic	4.35–4.93	0.9–3.4	1.07	Connection strength
Shahrooz et al. (2018)*	2	Cyclic	6.51	3.3	2.00	Coupling beam V_p
Kunwar and Shahrooz (2023)*	8	Cyclic	4.13–6.98	4.3–5.7	0.96-1.98	Connection strength

* Some or all specimens had auxiliary transfer bars.
+ Coupling beams in some specimens were solid sections or HSS (filled or unfilled)
d = Coupling beam depth
M_p = Plastic moment strength of the coupling beam
V_p = Plastic shear strength of the coupling beam

compiled, as provided in Table 1. Shahrooz et al. (1993) and Harries (1995) verified the applicability of Mattock-Gaffar's and Marcakis-Mitchell's equations for steel coupling beams subjected to cyclic loading. The controlling limit state in both studies was, however, either the plastic moment strength, M_p, or the plastic shear strength, V_p, of the steel coupling beam. Hence, the studies did not specifically evaluate the ultimate strength of the embedded connection. In several subsequent research programs, the connection strength had been enhanced by utilizing auxiliary transfer bars (reinforcing bars connected to the flanges to improve the bearing strength). Most of the past studies were focused on C-SSW in which the wall piers would be heavily reinforced and typically have boundary elements. A recent series of tests conducted by Kunwar and Shahrooz (2023) was focused on C-OSW with the connection strength being the controlling limit state. These tests demonstrated that the embedment length calculated by AISC 341-22, Equation H4-4 (Equation 1), was insufficient to develop the target member strength. To remedy the observed deficiency of Equation H4-4, a revised equation was developed by using basic principles in conjunction with relevant experimental data from the database, shown in Table 1. Derivation of the revised equation and its verification through test data and numerical simulations are presented in this paper.

DERIVATION OF A REVISED EQUATION

The database shown in Table 1 was filtered down to 10 specimens by focusing on (1) the tests with W-shapes that did not have auxiliary transfer bars, (2) those for which the connection strength was the controlling limit state, and (3) those with wall reinforcement similar to what would be placed in ordinary walls. The details of the 10 specimens are summarized in Table 2. Using the data from this table and the model shown in Figure 1, a revised equation for calculating embedment length was developed.

The bearing stress between the steel coupling beam flanges and the surrounding concrete was modeled according to Hognestad's (1951) concrete constitutive relationship that has a parabolic ascending branch and a linear post-peak descending branch. The peak concrete strength, f_c, was taken as $0.85\psi f'_c$ with ε_{01} and ε_{085} set equal to 0.002 and 0.0038, respectively. The selected value of 0.85 in the present derivation is intended to approximately account for nonuniformity of concrete compressive strength over the wall height. The bearing forces, C_f and C_b, were obtained by integrating the bearing stress distributed over the embedment length, L_e, and the coupling beam flange width, which was increased by a factor labeled α. This factor is intended to account for spreading of bearing stresses. Note that bearing stress is integrated over the depth of the neutral axis, c, to determine C_f and over $(L_e - c)$ for C_b.

The magnitude of applied shear, V, was incrementally increased, and the values of the strain at the wall-coupling beam interface, ε_f, and the depth of the neutral axis, c, were iterated until equilibrium of the vertical forces and moment could be achieved. The connection strength was taken as the maximum V for which equilibrium was possible. Figure 1(a) illustrates the case with $\varepsilon_f > \varepsilon_{01}$ and $\varepsilon_b < \varepsilon_{01}$; however, these strains were changed as needed in the iteration process.

During iteration, several options were considered to define the peak concrete strength (i.e., the value of coefficient ψ)

Table 2. Details of Specimens Used for Model Development											
Source	Specimen ID	Specimen Scale	b_w (in.)	b_f (in.)	d (in.)	g (in.)	L_e (in.)	L_e/d	Critical Mode	f'_c (ksi)	V_{test} (kips)
Mattock and Gaffar (1982)	W4	N/A	10.0	4.00	6.00	12.0	8.00	1.3	Shear	2.95	24.1
Kunwar and Shahrooz (2023)	SK-1	½	10.0	4.03	6.28	36.0	6.00	0.96	Flexure	4.13	14.2
	SK-2	½	10.0	4.03	6.28	36.0	7.00	1.1	Flexure	4.13	20.4
	SK-3	½	10.0	5.27	8.28	36.0	13.0	1.6	Flexure	6.95	49.0
	SK-4	½	10.0	5.27	8.28	36.0	13.0	1.6	Flexure	6.95	47.4
	SK-5	¾	15.0	8.05	12.1	54.0	19.0	1.6	Shear	6.98	109
	SK-6	¾	15.0	8.05	12.1	54.0	24.0	2.0	Shear	4.70	113
	SK-8	¾	15.0	8.05	12.1	54.0	19.0	1.6	Shear	6.15	89.7
Park et al. (2005) and Park and Yun (2006)	SCB-ST	⅓[a]	11.8	6.89	13.8	47.2	14.7	1.1	Flexure	4.93	70.4
	HCWS-ST	⅓[a]	11.8	6.89	13.8	47.2	14.7	1.1	Flexure	4.35	60.3

N/A: Could not be inferred due to inconsistencies between the cover to reinforcement and the other dimensions/bar sizes.
[a] Inferred based on the dimensions and bar sizes.

and the amount of spreading of bearing stresses (i.e., factor α). Finally, the most reasonably close match of the measured connection strength (V_{test} in Table 2) was found to be achieved by setting ψ equal to β_1 and taking α as the lesser of 1.3 and b_w/b_f, where b_w is wall pier thickness and b_f is coupling beam flange width.

The measured connection strengths are compared against those obtained from the final iteration (with $\psi = \beta_1$ and α = lesser of 1.3 and b_w/b_f) in Figure 2. The largest differences are for four cases (specimens SK-1, SK-2, SCB-ST, and HCWS-ST) with $L_e/d \leq 1.1$, where d is the depth of the coupling beam. For such cases, the embedment

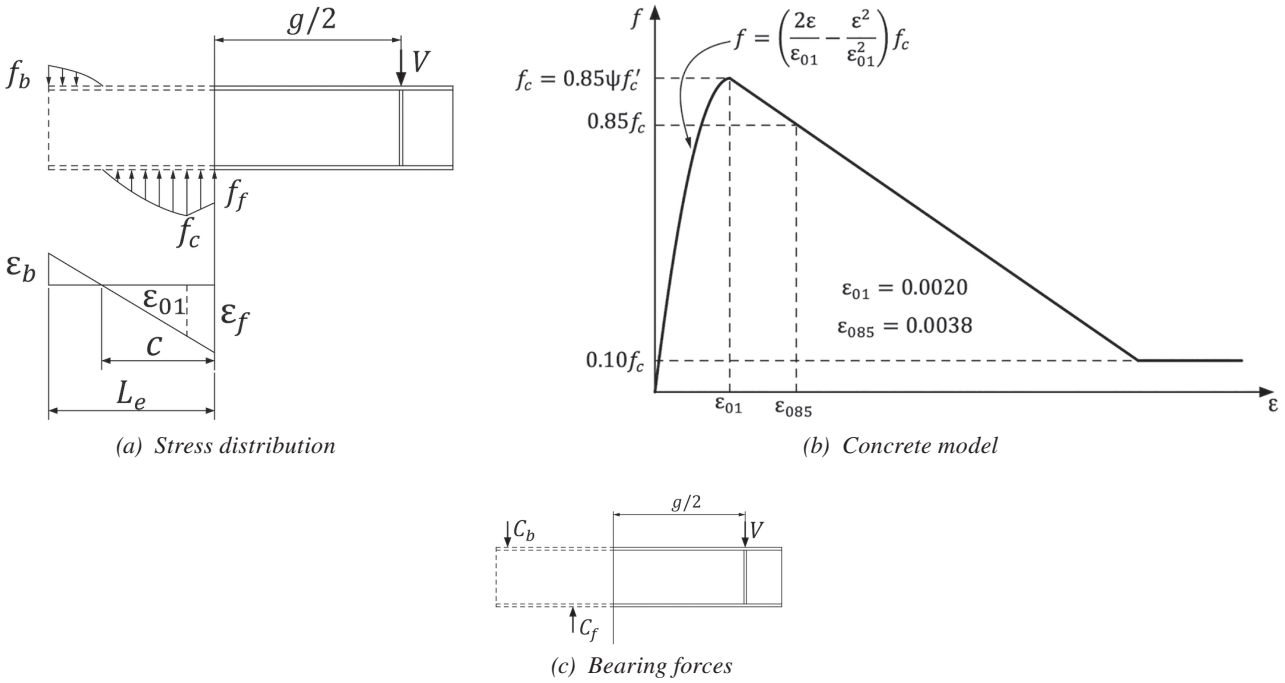

(a) Stress distribution

(b) Concrete model

(c) Bearing forces

Fig. 1. Assumed stress distribution and concrete model for development of revised equation.

Table 3. Values of ε_f and c/L_e after Iteration			
Source	**Specimen ID**	ε_f	c/L_e
Mattock and Gaffar (1982)	W4	0.0040	0.60
Kunwar and Shahrooz (2023)	SK-3	0.0038	0.57
	SK-4	0.0038	0.57
	SK-5	0.0037	0.56
	SK-6	0.0037	0.57
	SK-7	0.0036	0.56

region is characterized as a "D region," where the strain variation along the embedment length is more complex than the linear distribution shown in Figure 1(a), and the use of a strut-tie method is more appropriate (Kunwar and Shahrooz, 2023). Ignoring the cases with $L_e/d \le 1.1$, the measured connection strength is on average 1.17 times larger than the shear strength obtained from iteration with a coefficient of variation of 0.18.

Table 3 summarizes the values of ε_f and c/L_e (depth of the neutral axis normalized with respect to embedment length) corresponding to the values of V obtained from the final iteration, which are shown on the y-axis in Figure 2. As discussed previously, the strain is not distributed linearly along the embedment length for cases with L_e/d close to 1. Therefore, the results in Table 3 are provided only for the cases with $L_e/d > 1.1$. The average values of c/L_e and ε_f are 0.57 and 0.0038, respectively, with the corresponding coefficient of variation equal to 0.043 and 0.023. Setting $c/L_e = 0.57$ and $\varepsilon_f = 0.0038$ in the model depicted in Figure 1, Equation 2 was derived. Note that V_n, the nominal shear strength, in Equation 2 is the same as V shown in Figure 1 and used in the previous discussions. In this equation, α accounts for spreading of bearing stresses against the flanges.

$$V_n = \frac{0.19\alpha\beta_1 f_c' b_f L_e}{0.57 + \frac{g}{2L_e}} \quad \text{where } \alpha = \frac{b_w}{b_f} \le 1.3 \tag{2}$$

It should be noted that AISC 341-22, Equation H4-4 (Equation 1), was derived based on the average value of $c/L_e = 0.66$ and $\varepsilon_f = 0.003$ and bearing stress = $1.54\sqrt{f_c'}$. According to ACI 318-19, bearing stress is directly proportional to f_c' (and not $\sqrt{f_c'}$), which is consistent with the approach followed for the derivation of Equation 2. Spreading of bearing stresses in the current equation is represented by $(b_w/b_f)^{0.66}$.

EVALUATION OF REVISED EQUATION

The revised equation was evaluated by comparing the shear strengths calculated from Equation 2 versus the test results shown in Table 2. Additional comparisons were made

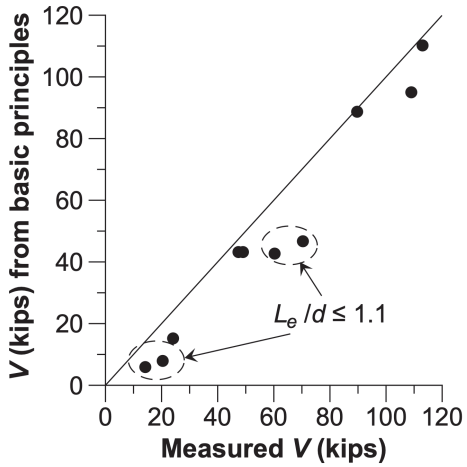

Fig. 2. Comparison of measured strengths and connection strengths from basic principles.

Table 4. Calculated Nominal Shear Strengths vs. Measured Values								
					$V_{n,\ calculated}$ (kips)		$V_{test}/V_{n,\ calculated}$	
Source	Specimen ID	L_e/d	Critical Mode	V_{test} (kips)	Current Equation	Revised Equation	Current Equation	Revised Equation
Mattock and Gaffar (1982)	W4	1.3	Shear	24.1	31.8	15.0	0.76	1.61
Kunwar and Shahrooz (2023)	SK-1	0.96	Flexure	14.2	11.8	5.8	1.20	2.44
	SK-2	1.1	Flexure	20.4	15.5	7.7	1.32	2.65
	SK-3	1.6	Flexure	49.0	55.9	42.1	0.88	1.16
	SK-4	1.6	Flexure	47.4	55.9	42.1	0.85	1.12
	SK-5	1.6	Shear	109	122	92.7	0.90	1.18
	SK-6	2.0	Shear	113	159	109	0.71	1.04
	SK-7	1.6	Shear	89.7	118	86.4	0.76	1.04
Park et al. (2005)	SCB-ST	1.1	Flexure	70.4	64.4	45.5	1.09	1.55
	HCWS-ST	1.1	Flexure	60.3	61.8	41.6	0.98	1.45

Table 5. Comparison of Embedment Lengths for Test Specimens				
		Calculated L_e (in.)		
Source	Specimen ID	Current Equation	Revised Equation	% Increase
Mattock and Gaffar (1982)	W4	7	15	114%
Kunwar and Shahrooz (2023)	SK-1	7	14	100%
	SK-2	9	17	89%
	SK-3	12	17	42%
	SK-4	12	16	33%
	SK-5	18	24	33%
	SK-6	20	29	45%
	SK-7	17	23	35%
Park et al. (2005)	SCB-ST	16	22	38%
	HCWS-ST	15	22	47%

through numerical simulations of more than 12,000 cases. Moreover, the embedment lengths determined from the revised and current equations were compared.

Based on Test Results

Using the dimensions and measured properties provided in Table 2, the nominal shear strengths, V_n, were computed from the revised equation (Equation 2) and the current AISC 341-22, Equation H4-4 (Equation 1). The results are compared against their experimental counterparts in Table 4. The nominal strengths instead of reduced design strengths, ϕV_n, are compared because the test specimens had been fabricated under controlled conditions, the as-built dimensions and measured material properties were used in the calculations, and the loading was well defined and known *a priori*. There is no obvious correlation between whether the coupling beam is shear/flexure critical and if the measured strength is overestimated or underestimated by the current equation. For example, specimens SK1 to SK4 were flexure controlled; however, SK1 and SK2 could develop V_n calculated from the current equation but SK3 and SK4 could not. None of the shear-controlled specimens could reach the V_n from the current equation. A common factor is the embedment region "aspect ratio"—that is, L_e/d.

For specimens SK-1, SK-2, SCB-ST, and HCWS-ST with small values of L_e/d, the measured connection strength is

Table 6. Values for Parametric Cases	
Variable	**Range/Value**
Size of coupling beam	W14×22 to W30×326 excluding sections heavier than 350 plf
Wall thickness, b_w	18 in. to 54 in. (2 in. increment) Ignore cases with $b_w/b_f > 2$
Span of coupling beam, g	4 ft to 10 ft (1 ft increment)
Concrete compressive strength, f'_c	4 to 10 ksi (1 ksi increment)
Design shear, V	Smaller of $0.95(2\phi_b M_n/g$ and $\phi_v V_n)$ with no R_y
Wall transverse reinforcement	#5 with ¾ in. cover
Wall longitudinal reinforcement	#10

nearly equal to or larger than the nominal shear strength calculated by either the current or revised equation. It is reemphasized that the underlying assumption (a linear strain distribution over the embedment length) used for the derivation of both equations is not appropriate when L_e/d is small. The current equation, on the other hand, overestimates the measured connection strength (i.e., it underestimates the embedment length required to develop V_n) in 6 out of 10 cases with L_e/d greater than 1.1, including specimen W4 used by Mattock and Gaffar (1982) in the derivation of the current equation. The average value of $V_{test}/V_{n,current\ Eq.}$ is 0.81 with a coefficient of variation of 0.093. In contrast, the revised equation provides reasonable and conservative values. All the strength ratios from the revised equation are greater than 1. For the cases with L_e/d greater than 1.1, the average value of test/calculated nominal connection shear strength is 1.19 with a coefficient of variation equal to 0.18.

The required embedment lengths to develop the measured connection strengths (V_{test} shown in Table 4) were computed by using the current Equation 1 and the revised Equation 2 and are compared in Table 5. The calculated embedment lengths were rounded to the nearest in. Compared to the existing equation, the embedment length from the revised is, on average, 50% longer for cases with L_e/d greater than 1.1.

Based on Numerical Simulations

The revised equation was further evaluated numerically by considering a wide range of the key parameters: b_f, b_w/b_f, f'_c, and g. For this purpose, a total of 12,054 cases were selected based on the variables shown in Table 6. For a given wall thickness, the beam sizes were selected such that there would be a minimum of a 1 in. gap on either side of the beam flange and wall longitudinal bars. This gap is somewhat arbitrary but is the same as the value in ACI 318-19 for the minimum distance between longitudinal bars to ensure concrete consolidation. The concrete compressive strength was capped at 10 ksi to be consistent with the current AISC limit.

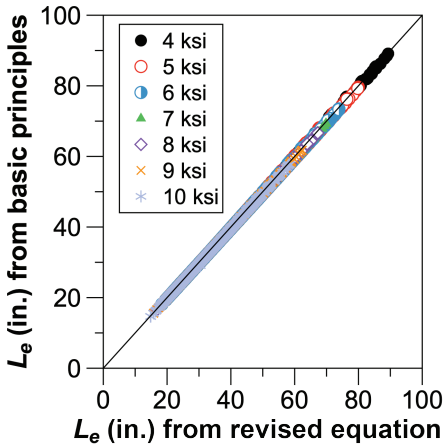

Fig. 3. Embedment length calculated from basic principles and revised equation.

The model shown in Figure 1 was used with the same assumptions used for derivation of Equation 2: (1) ε_f was set equal to 0.0038 and (2) spreading of bearing stresses was taken into account by multiplying the flange width by a taken as the lesser of 1.3 and b_w/b_f. The values of the depth of the neutral axis, c, and embedment length, L_e, were iterated to maintain equilibrium for a given value of design shear taken as the smaller of $0.95(2\phi_b M_n/g$ and $\phi_v V_n)$.

The analyses indicate that c/L_e ranges between 0.53 and 0.64, but Equation 2 was developed based on setting c/L_e equal to 0.57. This difference does not noticeably affect the calculated embedment lengths as evident from Figure 3, which compares the embedment length determined from basic principles (i.e., satisfying equilibrium of forces and moment by iterating the values of c and L_e) and the value calculated from Equation 2. Out of 12,504 cases, the embedment length determined from basic principles is longer than the value determined from Equation 2 for 91, 32, 14, 5, and 5 cases with f_c' equal to 4 ksi, 5 ksi, 6 ksi, 7 ksi, and 8 ksi, respectively. The largest difference is 0.82% for a case involving a 4-ft-long W18×311 beam used to couple 4 ksi wall piers. The application of such a heavy section to couple 4 ksi wall piers is not considered to be likely. The revised equation is, hence, deemed to be applicable for a wide range of cases encountered in practice.

The application of AISC 341-22, Equation H4-4 (Equation 1), to cases with relatively high concrete strengths is somewhat questionable considering the value of f_c' was 2.95 ksi for the only W-shape section used in the original research (Mattock and Gaffar, 1982). The current equation has been examined in several research programs with larger values of f_c', but the connection strength was not the controlling failure mode, the value of L_e/d was such that the underlying assumption of linear strain distribution along embedment length would not be accurate, or the connection strength was found to be less than the target strength. Nevertheless, the embedment lengths for the aforementioned 12,504 cases were calculated by the current equation, Equation 1, and the revised Equation 2, and the results were compared.

The histogram of the ratio of embedment length, L_e, from the revised equation divided by that from the current equation is plotted in Figure 4. On average, the embedment length calculated from the revised equation is 1.15 times longer than that from the current equation with a coefficient of variation of 0.078. The revised equation results in a maximum of 37% longer embedment length compared to the current equation. The embedment length from the current equation is slightly longer than that from the revised equation for a limited number of cases involving large concrete compressive strengths: 0.08%, 0.74%, and 2.54% of the number of cases with $f_c' = 8$ ksi, 9 ksi, and 10 ksi, respectively. However, the ratio of L_e from the revised equation to that from the current equation is 0.97 or larger for 99.2% of the total number of cases.

In addition to concrete compressive strength, the value of b_w/b_f, the coupling beam unit weight, and the expected yielding sequence (shear-critical, flexure-critical, or simultaneous yielding in flexure and shear) affect the relative magnitudes of embedment length from the revised and current equations, as evident from Figure 5. The ratio of embedment length from the revised equation to the length from the current equation drops below 1 for cases with f_c' exceeding 8 ksi, and as b_w/b_f becomes small, the coupling beam becomes heavier, and the coupling beam is shear critical (i.e., $g \leq 1.6M_p/V_p$) or is expected to yield in flexure and shear simultaneously (i.e., $1.6M_p/V_p < g < 2.6M_p/V_p$). It is noted again that the application of the current equation to cases with large values of f_c' is questionable.

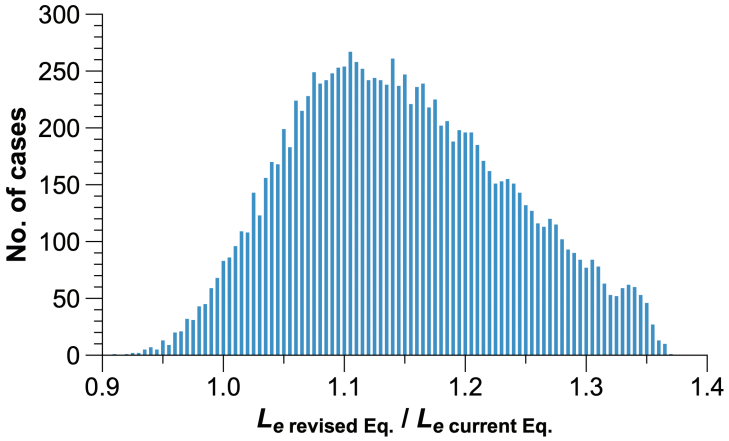

Fig. 4. Comparison of embedment lengths.

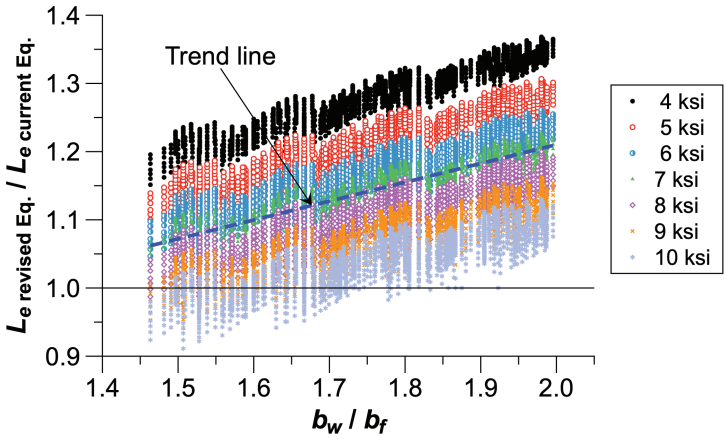

(a) Influence of b_w/b_f

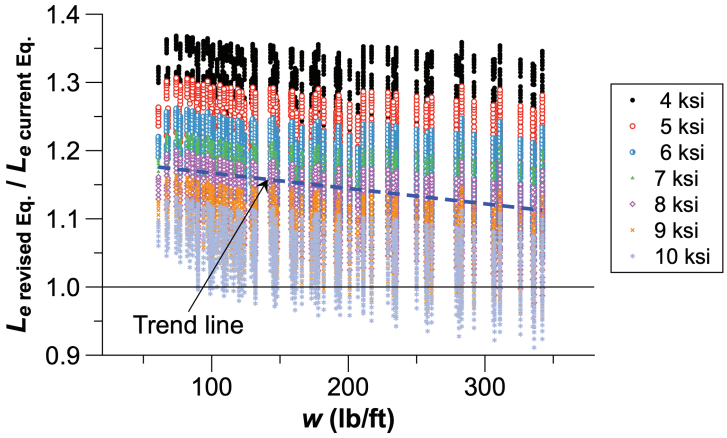

(b) Influence of coupling beam weight/foot

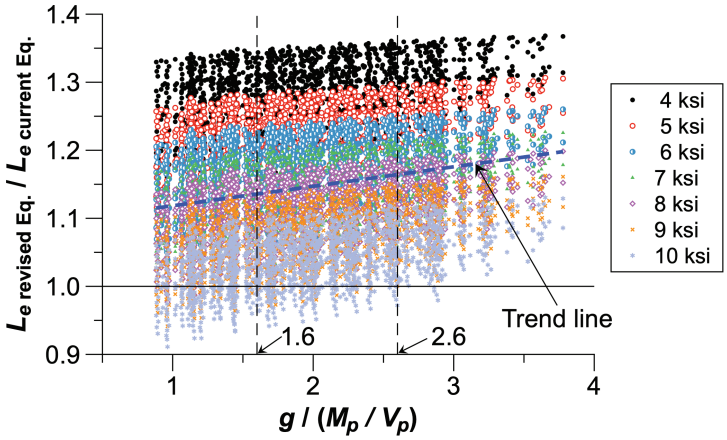

(c) Influence of yielding sequence

Fig. 5. Influence of various parameters on embedment length from revised equation vs. current equation.

CONCLUSION

Recent tests focused on steel coupling beams in composite ordinary shear walls (C-OSW) demonstrated the target strength could not be developed for several test specimens designed according to the current embedment length equation in AISC 341-22. A revised equation was developed and evaluated by using basic principles in conjunction with available test data. The equation was further validated through numerical simulations. The revised equation results in longer embedment lengths by as much as nearly 40% for cases that would likely be encountered in practice. The longer embedment length will ensure that the design loads can be developed prior to connection failure in the embedded region. The revised equation presented herein as Equation 2 is being considered as a replacement for the current AISC 341-22, Equation H4-4.

ACKNOWLEDGMENTS

The research presented in this report was funded by the Charles Pankow Foundation and co-funded by the American Institute of Steel Construction and the Magnusson Klemencic Associates (MKA) Foundation. The views presented in this paper are of the authors and do not represent the funding agencies' views. The authors dedicate this paper to our friend and colleague, Dr. Patrick J. Fortney at the University of Cincinnati, who unexpectedly passed away in 2019. His deep desire to understand the behavior and performance of ordinary composite coupled walls was the genesis of the reported research.

REFERENCES

ACI (2019), *Building Code Requirements for Structural Concrete*, ACI 318-19R and commentary, Farmington Hills, Mich.

AISC (2022), *Seismic Provisions for Structural Steel Buildings*, ANSI/AISC 341-22, American Institute of Steel Construction Chicago, Ill.

Fortney, J.P. (2005), "The Next Generation of Coupling Beams," PhD Dissertation, University of Cincinnati, Cincinnati, Ohio.

Harries, K.A. (1995), "Seismic Design and Retrofit of Coupled Walls Using Structural Steel," PhD Dissertation, McGill University, Montreal, Quebec, Canada.

Hognestad, E. (1951), "A Study of Combined Bending Axial Load in Reinforced Concrete Members," Bulletin Series No. 399, Engineering Experimental Station, University of Illinois, Urbana, Ill.

Kunwar, S. and Shahrooz, B.M. (2023), "Steel Coupling Beams in Low-Seismic and Wind Applications," Final Report to the Charles Pankow Foundation.

Marcakis, K. and Mitchell, D. (1980), "Precast Concrete Connections with Embedded Steel Members," *PCI Journal*, Vol. 25, No. 4, pp. 88–116.

Mattock, A.H. and Gaafar, G.H. (1982), "Strength of Embedded Steel Sections as Brackets," *ACI Structural Journal*, Vol. 79, No. 2, pp. 83–93.

Park, W.S. and Yun, H.D. (2006), "Seismic Performance of Steel Coupling Beam–Wall Connections in Panel Shear Failure," *Journal of Constructional Steel Research*, Vol. 62, pp. 1,016–1,025.

Park, W.S., Yun, H.D., Hwang, S.K., Han, B.C., and Yang, I.S. (2005), "Shear Strength of the Connection between a Steel Coupling Beam and a Reinforced Concrete Shear Wall in a Hybrid Wall System," *Journal of Constructional Steel Research*, Vol. 61, pp. 912–941.

Shahrooz, B.M., Fortney, P.J., and Harries, K.A. (2018), "Steel Coupling Beams with a Replaceable Fuse," *Journal of Structural Engineering*, ASCE, Vol. 144, No. 2, 04017210_1:11.

Shahrooz, B.M., Remmetter, M.E., and Qin, F. (1993), "Seismic Design and Performance of Composite Coupled Walls," *Journal of Structural Engineering*, ASCE, Vol. 119, No. 1, pp. 3,291–3,309.